Analysis and Experimentation with Dissipative Nonlinear Controllers for Series Resonant DC/DC Converters

A. M. Stanković † **D.J. Perreault ‡** **K. Sato ‡**

†Department of Electrical and Computer Engineering
Northeastern University, Boston, U.S.A.
‡Laboratory for Electromagnetic and Electronic Systems
Department of Electrical Engineering and Computer Science
M.I.T., Cambridge, U.S.A.

Abstract - The paper describes practical experience and analytical advances in a nonlinear controller design methodology for series resonant DC/DC converters. The control goal is to maintain the output voltage in the presence of large load perturbations by varying the switching frequency. The proposed methodology utilizes large scale, nonlinear switched and generalized averaged models, and the resulting closed-loop system is exponentially convergent under typical operating conditions. The designer has a direct handle over the convergence rate, and the nonlinear controller requires only the usual output voltage measurements, while the load variations are estimated. In this paper, the previously reported results are extended in two directions: 1) a dissipativity-based nonlinear controller is implemented in affordable analog circuitry, and evaluated experimentally; 2) the control structure is generalized to allow for both resistive and current loads.

I. INTRODUCTION

The literature on modeling and control of resonant converters is voluminous, and we list only references directly related to our development. Control-oriented modeling of resonant converters using the generalized averaging procedure has been addressed in [1, 2, 3]. Small-signal models for series and parallel resonant converters have been derived and verified in [4]. A linear control law using the energy stored in the resonant tank has been developed in [5]. A controller that traverses an optimal trajectory in terms of the resonant tank variables has been described in [6]. Sampled-data modeling and digital control of a series resonant converter has been addressed in [7]. The use of physical and circuit-theoretic properties such as dissipativity in control design of switched-mode power converters has been suggested in [8, 9], together with Lyapunov-based techniques utilizing "energy in the increment". This paper proceeds along a similar direction, and employs a generalization of the dissipativity-based design procedure for series resonant DC/DC converters given in [10]. The procedure described in this paper allows for for both resistive and current loads, and is verified in laboratory experiments that employ simple analog hardware.

The standard controller structure for a series resonant DC/DC converter is a fixed linear PI controller whose input is the deviation in the output voltage, and whose output is the change in switching frequency. This controller has the advantages of being simple to design and easy to implement. Its main disadvantage is a fairly low closed-loop bandwidth (for converters with switching frequency of the order of 50 kHz the closed-loop bandwidth rarely exceeds 20 Hz). It was shown in [11] that this problem is not accidental, as uncertainties introduced by load variations prevent the PI structure (and other fixed, linear controllers) from providing both robust stability and robust performance.

The main control design approach advanced in this paper is to "shape" the total energy of the closed-loop system, while achieving output voltage regulation. Our methodology differs from the feedback linearization and similar approaches as it avoids some intrinsically non-robust operations, such as exact cancellations of nonlinearities. Our control approach utilizes the physical laws underlying energy conversion and the model structure in a fundamental way, as it consists of: 1) specification of the desired (target) total energy function of the closed-loop system, and desired (periodic) steady-state trajectories that provide output voltage regulation, 2) addition of "damping" around this nominal trajectory (i.e., dissipation of undesirable deviations of stored energy) that assures exponential convergence towards the nominal trajectory, thus guaranteeing robust operation. While the basic dissipativity-based control design methodology assumes measurements of all states and disturbances, an improvement that estimates the unknown, but constant (parametric) disturbance [12, 10] is applied to resonant DC/DC converters in this paper.

The paper is organized as follows: in Section II a mathematical model of the series resonant converter is presented; in Section III a dissipativity-based control law is designed; simulations and laboratory tests are described

0-7803-3840-5/97/$10.00 © 1997 IEEE

in Section IV, while conclusions are outlined in Section V; remarks concerning the differential flatness property of a series resonant converter are presented in the Appendix.

II. Modeling a Series Resonant Converter

A series resonant DC/DC converter is shown in Fig. 1. Using the notation given in the figure, a state-space model

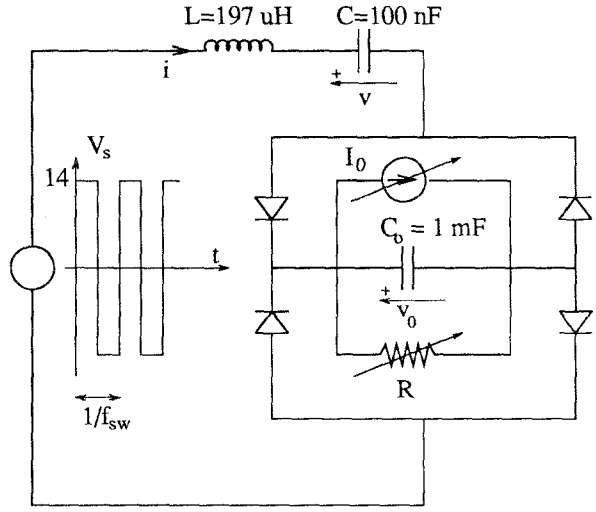

Figure 1: Circuit schematic of a series resonant converter

can be written as:

$$\begin{aligned} L\frac{di}{dt} &= -v - v_0\, sgn(i) + V_s\, sgn(\sin(\omega_s t)) \\ C\frac{dv}{dt} &= i \\ C_0\frac{dv_0}{dt} &= abs(i) - \frac{v_0}{R} - I_0 \end{aligned} \tag{1}$$

where ω_s denotes the switching frequency in rad/sec, v and i are the resonant tank voltage and current respectively, v_0 is the output voltage supplying the load comprising a resistor R and a current sink I_0.

An application of the energy-shaping idea is not straightforward, as nominal, periodic state waveforms that achieve the output tracking are not apparent. Instead, we apply the generalized averaging procedure introduced in [1] to model (1). In particular, we assume that both v and i are described with sufficient accuracy when their first (time-varying) harmonics are retained (denoted with V_1 and $I_1 = |I_1|e^{j\psi}$, respectively), while v_0 is assumed to be a DC quantity. It has been observed both experimentally and in numerical simulations that these assumptions are reasonable in well designed DC/DC series resonant converters [1, 11]. A (nonlinear) model for the dynamics of local harmonics is then obtained [1]:

$$\begin{aligned} \frac{dI_1}{dt} &= -j\,\omega_s\, I_1 + \frac{1}{L}(-V_1 - \frac{2}{\pi}V_0 e^{j\psi} - j\frac{2\,V_s}{\pi}) \\ \frac{dV_1}{dt} &= -j\,\omega_s\, V_1 + \frac{1}{L}\, I_1 \\ \frac{dV_0}{dt} &= \frac{4}{C_0\pi}abs(I_1) - \frac{V_0}{R\,C_0}. \end{aligned} \tag{2}$$

This model can be written in the form of a fifth order model involving real valued quantities, for example by taking real and imaginary parts of the first two equations. Let $I_1 = x_1 + jx_2$, $V_1 = x_3 + jx_4$ and $V_0 = x_5$. The control input is the switching frequency $\omega_s = u_1$ (and possibly the supply voltage $V_s = u_2$); we define the outputs of interest to be magnitude of the DC output y_1 (and possibly magnitudes of the series tank current, denoted by y_2, and voltage, denoted by y_2). Then the model (2) becomes

$$\begin{aligned} \frac{dx_1}{dt} &= x_2\, u_1 - \frac{x_3}{L} - \frac{2x_5}{\pi L}\frac{x_1}{\sqrt{x_1^2+x_2^2}} \\ \frac{dx_2}{dt} &= -x_1\, u_1 - \frac{x_4}{L} - \frac{2x_5}{\pi L}\frac{x_2}{\sqrt{x_1^2+x_2^2}} - \frac{2u_2}{\pi L} \\ \frac{dx_3}{dt} &= x_4\, u_1 + \frac{x_1}{C} \\ \frac{dx_4}{dt} &= -x_3\, u_1 + \frac{x_2}{C} \\ \frac{dx_5}{dt} &= \frac{4}{\pi C_0}\sqrt{x_1^2+x_2^2} - \frac{x_5}{C_0\,R} - \frac{I_0}{C_0} \\ y_1 &= x_5 \\ y_2 &= \sqrt{x_1^2+x_2^2} \\ y_3 &= \sqrt{x_3^2+x_4^2} \end{aligned} \tag{3}$$

For control design purposes we will consider the linearization of this model (denoted with $\tilde{x}$,$\tilde{u}$ and $\tilde{y}$) around an equilibrium operating point (denoted with X,U and Y) corresponding to fixed switching frequency and supply voltage. In the calculation of equilibrium quantities the phasor diagram given in Fig. 2 is useful. Analysis of (2) in a steady state yields

$$|\, I_1 \,| = \omega_s\, C\ |\, V_1 \,|$$

and

$$X_5 = V_{0,ss} = \frac{4R}{\pi}\,|\, I_1 \,|\,.$$

Using Pythagoras theorem in the phasor diagram in Fig. 2, we obtain

$$|\, V_1 \,|^2\,[(1 - LC\omega_s^2)^2 + (\frac{8R}{\pi^2}\omega_s C)^2] = (\frac{2V_s}{\pi})^2.$$

Now we are in a position to calculate the small-signal model corresponding to equation (3) around any equilibrium point using standard linearization procedures.

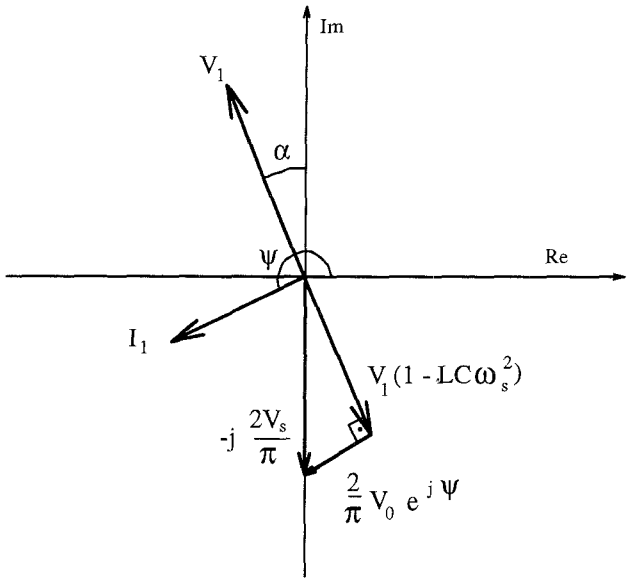

Figure 2: Current and voltage phasor diagram at an equilibrium.

In Figs. 3 and 4 we present the Bode magnitude and phase plots, respectively, from the deviations in *normalized* switching frequency (in per unit of the resonant frequency) to the deviations in the output DC voltage (cf [4]). The loads of interest are minimal R (1Ω), nominal R (1.6Ω), a typical low load (6Ω) and the maximal R (50 Ω, "no–load" condition). We note large variations

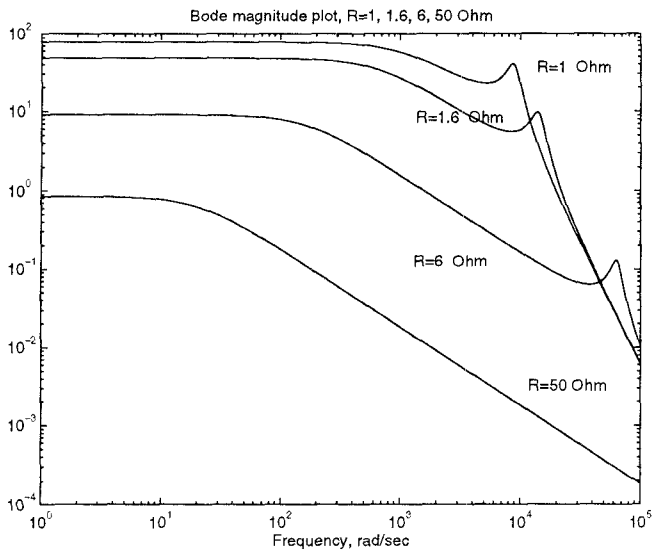

Figure 3: Bode magnitude plots for various loads

in the linearized model due to loading changes, motivating the use of robust controller design techniques. These variations prevent fixed linear compensators (of reasonable complexity) from achieving good performance over the whole operating range. Observe that the resonant

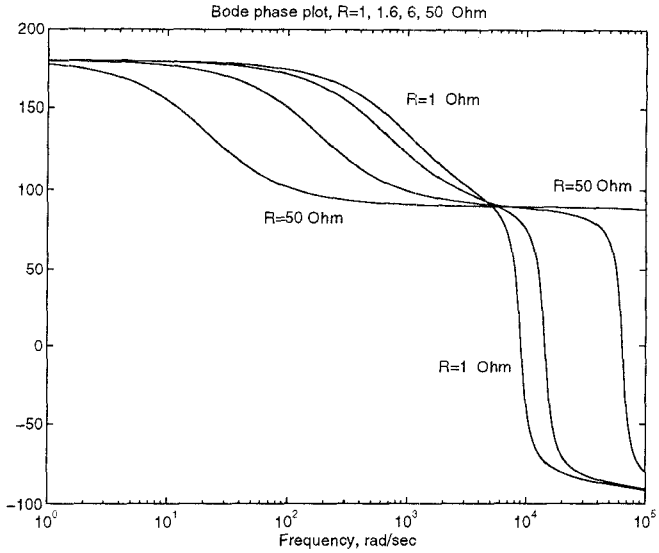

Figure 4: Bode phase plots for various loads

peaks in the magnitude plots correspond to the difference of the resonant frequency ω_0 and the switching frequency ω_s, emphasizing the need for considering performance robustness.

III. Design of a Control Law

Our qualitative analysis of dynamics in a series resonant DC/DC converter is based on the fact that typically variations in the tank variables are usually much faster than changes in the output voltage (this property has been quantified in [10]). Motivated by this reasoning, we follow [10] in assuming that the transients in the tank variables are instantaneous relative to the output voltage. The first step of control design is then to shape the energy stored in the output capacitor assuming the magnitude of the first harmonic of the tank current as a pseudo control input. Given the required value of the tank current, on the second step we evaluate the corresponding switching frequency using the steady–state relationship between the switching frequency and the magnitude of the tank current.

Let $G = 1/R$ denote the conductance of the resistive load, and let $\hat{(\cdot)}$ denote an estimate of $(\cdot)$. Then, for a given reference (desired) value of the output voltage $V_{0,d}$, we define the error signal $e = (v_0 - V_{0,d})$, and consider the energy function

$$H_d = (1/2)C_0 e^2 + \frac{V_{0,d}}{2g}(\hat{G} - G)^2 + \frac{1}{2h}(\hat{I}_0 - I_0)^2 \qquad (4)$$

where g and h are positive (design) constants that are used to generate the load estimates from the available output

voltage measurement:

$$\frac{d\hat{G}}{dt} = -ge,$$

and

$$\frac{d\hat{I}_0}{dt} = -he.$$

The control design task is thus to find the pseudo-control input $|I_{1,d}|$ to guarantee

$$\dot{H}_d \leq -(G + k_{dis})e^2, \tag{5}$$

where k_{dis} is another positive design constant. Direct calculations show that this goal is achieved by setting

$$|I_{1,d}| = \max(\frac{\pi}{4}(V_{0,d}\hat{G} + \hat{I}_0) - k_{dis}e, 0).$$

Given the pseudo-control $|I_{1,d}|$, we evaluate the actual control (switching frequency) using the relationship which follows from the relationships derived for the sinusoidal steady state:

$$| I_1 |^2 (1 - LC\omega_s^2)^2 = (\omega_s C)\frac{4}{\pi^2}(V_s^2 - V_{0d}^2). \tag{6}$$

Note that this control policy establishes exponential convergence of the output voltage to its desired value. Due to issues of observability, we can not guarantee that the estimates of load parameters ($\hat{G}$ and $\hat{I}_0$) used in deriving the required control input will converge to their true values. This convergence does, however, take place when only one of the parameters is estimated (and the other one is known).

IV. Simulations and Laboratory Tests

To illustrate our design approach we use the example from [1] with parameter values $L = 197\mu$H, $C = 100n$F, (yielding the resonant frequency of $\omega_0 = 2\pi \cdot 35,860$), $C_0 = 1m$F, $V_s = 14$V. In the case of purely resistive load, the nominal load resistance is $R = 1.6\Omega$, $\omega_s = 2\pi \cdot 38,110$ rad/sec (corresponding to $v_0 = 3.26$V, $| V_1 | = 70.25$V, $| I_1 | = 1.68$A and $\psi = 194.1^o$). In the case of a mixed load, $I_0 = 1$A and $R = 10\Omega$. We assume that the system initially operates at the nominal equilibrium, and then we explore effects of changes in load from the nominal value: 1) large load deviation (R steps to 5Ω, a 90% reduction, or I_0 steps to 0.3 A, a 70% reduction); 2) very large load deviation in which R steps to 50 Ω (99.9% load reduction, an almost complete load rejection). For simulation purposes the nonlinear model (2) has been implemented in the Simulink environment.

The controller requires load estimates $\hat{G}$ and $\hat{I}_0$ that can be readily produced with a single integrator, and the pseudo control $|I_1|$ can be calculated using simple circuit elements. The main challenge in a circuit implementation is in producing the switching frequency ω_s from the known (fourth-order) steady-state relationship (6). We have addressed this issue by developing an approximation to the functional dependence (6) of ω_s from $|I_1|$. Our approximation consists of three straight line segments, and it is implemented with three operational amplifier circuits.

In Fig. 5 we overlay the *experimental* results for the output voltage (solid line, down-loaded from a digitizing oscilloscope) with our simulation results (that are based on (6), with $g = 150$ and $k_{dis} = 1$, and not on the three line approximation). The transient is initialized by the load change from $R = 1.6\Omega$ to $R = 5\Omega$. We note a good overall agreement, with the differences being attributable to approximations in our circuit implementation. The closed-loop bandwidth is in the order of 300 Hz, and the complexity of this implementation compares favorably even with linear controllers.

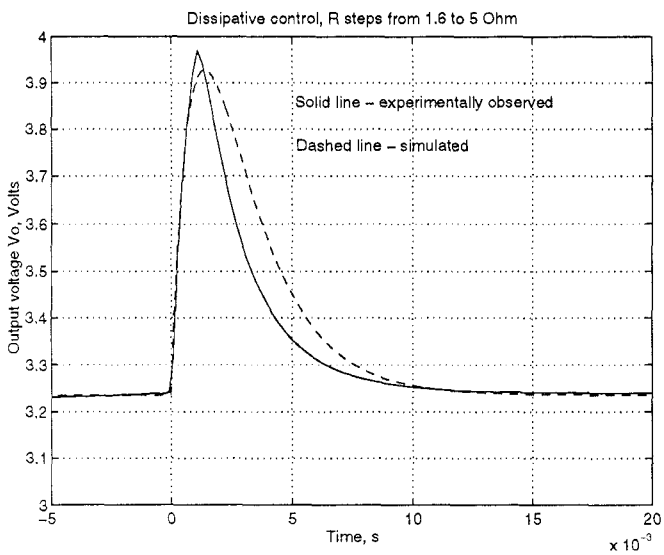

Figure 5: Comparison between experimentally observed and simulated transient in v_0, for a resistive load.

Next, we compare the performance of the dissipativity-based controller with simulations with two fixed linear controllers from [11] that are presented in Fig. 6. One of the controllers is a PI controller with transfer function $190/(s + 0.01)$, while the other is a lead-type controller obtained through a Quantitative Feedback Theory (QFT) design methodology $3232(s+818.4)/(s+0.01)(s+233.3 \times 10^3)$. To make the comparison fair, in both designs we aim to obtain a fast closed-loop response. Note that the speed with which deviations in the output voltage can be eliminated is inherently limited by the output resistance forming a parallel RC_o combination, and this is es-

pecially pronounced for large R. The PI controller results in a more oscillatory response, but with smaller excursions of the output voltage [11] (in both cases the closed–loop bandwidth is of the order of 50 Hz).

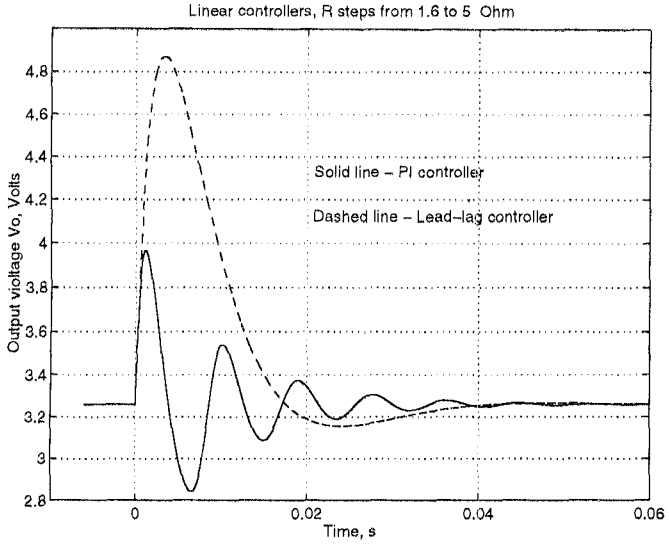

Figure 6: Simulated responses with linear controllers: PI (solid line) and lead controller (dashed line).

Turning our attention to the case of a current load, in Fig. 7 we overlay the experimental results for the output voltage (solid line, down-loaded from a digitizing oscilloscope) with our simulation results (that are based on (6), with $h = 500$ and $k_{dis} = 1$). The transient is initialized by the load change from $I_0 = 1$A to $I_0 = 0.3$A, with a constant resistive part $R = 10\Omega$. We note a good overall agreement, with the differences again being attributable to approximations in our circuit implementation. The closed–loop bandwidth is of the order of 400 Hz.

Finally, we consider very large load changes in which load steps from 1.6 Ω to 50 Ω (99.9 % load rejection). In Fig. 8 we compare the experimental results for the output voltage (solid line) with our simulation results (that are based on (6), with $g = 150$ and $k_{dis} = 1$, and not on the three line approximation). The overall agreement, especially in terms of voltage excursion, is quite good; the approximations used in the circuit implementation figure prominently in the second part of the transient. The closed–loop bandwidth is in the order of 100 Hz. Next, we compare the performance of the dissipativity–based controller with simulations using the two fixed linear controllers that are presented in Fig. 9. Observe that the closed–loop bandwidth of the linear controllers is below 10 Hz.

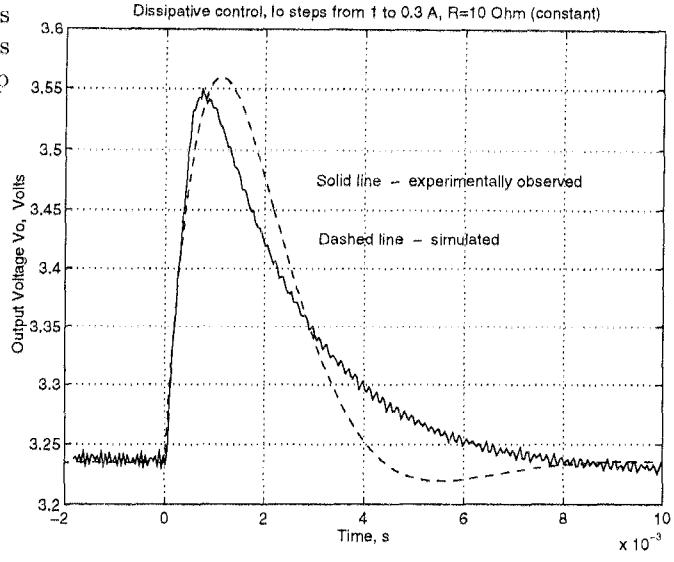

Figure 7: Comparison between experimentally observed and simulated transient in v_0, for a current load.

V. Conclusions

The control design approach presented in this paper utilizes physical insights (such as energy dissipativity) in both modeling and control synthesis, as well as time–scale separation in deriving a controller. The resulting closed–loop system is inherently robust with respect to uncertainties compatible with the underlying physical processes, as we have demonstrated in our experiments. The proposed dissipativity-based nonlinear controller yields a performance that is greatly improved when compared to the class of linear fixed compensators: 1) the duration of a transient is decreased close to an order of magnitude, and 2) the size of the output voltage excursion is less than half of the one achievable with linear compensators of comparable complexity. The closed–loop bandwidth of dissipativity–based controllers is limited by the domain of validity of the assumed model (in which resonant tank variables are assumed to be much faster than the output voltage), and by the quality of measurements of the output voltage.

Appendix

The controller presented in this paper is an example of the "two degree of freedom" control design approach: the synthesis problem is separated into 1) design of a feasible trajectory for the nominal model, and 2) regulation around that trajectory using controllers that have guaranteed performance in the presence of uncertainties and disturbances. This approach is particularly well suited for differentially flat systems: in practical terms, a system is

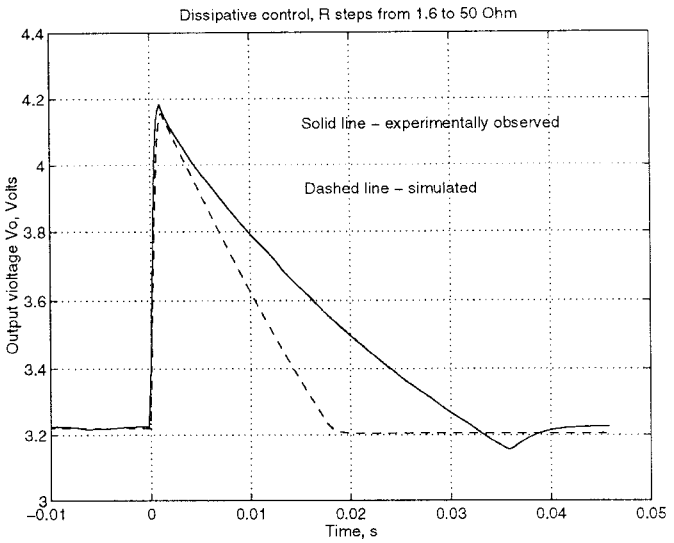

Figure 8: Comparison between experimentally observed and simulated transient in v_0, for a very large change in resistive load.

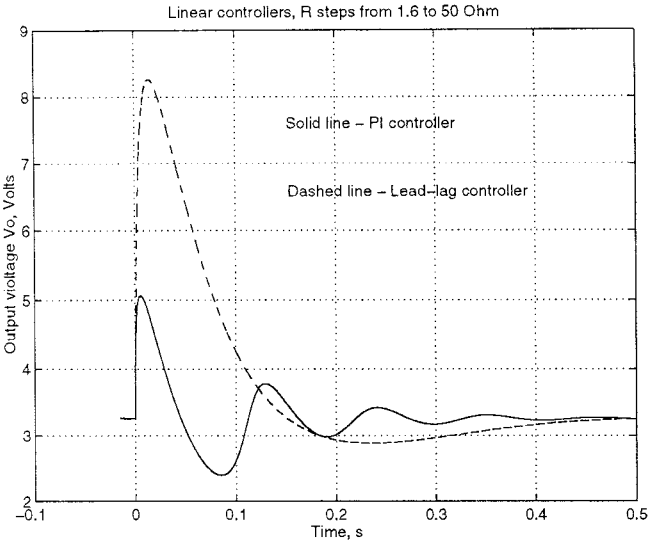

Figure 9: Simulated responses of a very large transient with linear controllers: PI (solid line) and lead controller (dashed line).

differentially flat if a set of outputs can be found (equal in number to the number of inputs) so that all states and inputs can be determined using only algebraic relationships and differentiation [13] (note that the choice of outputs is unrestricted). While the numerical differentiation is to be avoided in practice due to noise amplification, the property of flatness often translates into availability of computationally attractive algorithms. In the case of linear systems, the differential flatness is equivalent to controllability. There are, however, no systematic procedures for determining flatness of nonlinear dynamical models at this time. The differential flatness of second order models of switched mode converters (boost and buck-boost), and their cascades has been addressed in [14].

If we consider the model of a series resonant converter in which resonant tank dynamics are assumed to be instantaneous ("singularly perturbed" case [10]), then it turns out to be differentially flat. For simplicity, we analyze the case with a purely resistive load. Consider the open–loop operation first: there are two inputs – control input ω_s and the disturbance input $G = 1/R$; take the output voltage as the first output, and the disturbance input G as the second output. Then from the first output, its derivative and the second output (and known circuit parameters) we can determine the magnitude of the tank current; from the memoryless nonlinearity (6), we can determine the control input ω_s. In the case of closed–loop operation with a dissipative controller, we have one input (the disturbance G); we take the estimate $\hat{G}$ as our flat output. By differentiating this output we find $e = v_0 - V_{0,d}$, the output voltage v_0 and its derivative. From $\hat{G}$ and known controller parameters we can find ω_s and the resonant tank current $|I_1|$. Finally, from the equation for the output stage, we find G (satisfying $G \geq 0$).

The more detailed model (3) of the system appears not to be flat. An indication can be found in the linearized model as it is not controllable, and the transfer function from ω_s to v_0 has two (non–minimum phase) zeros, indicating impossibility of completely recovering the control input from the output voltage. If, however, we additionally assume that ω_s is measured, then in the open–loop operation and for typical circuit parameter values we can recover all states (and the magnitude of the input voltage V_s, if it is an additional control input). We pick the outputs as in the case of the model with no tank dynamics; from the last equation in (2) and v_0 and $\dot{v}_0$, we find $\sqrt{x_1^2 + x_2^2}$ and $x_1^2 + x_2^2$ (assuming the nonzero tank current throughout); we additionally assume that the ratio of rates of change of energies stored in the tank inductor and capacitor equals the ratio $(\omega_s/\omega_0)^2$ of stored energies in these elements at an equilibrium. This assumption holds very well in our example, even during very large transients (and both rates are very small compared to the source and load powers). Thus, $Ld(x_1^2 + x_2^2)/dt = (\omega_s/\omega_0)^2(x_1x_3 + x_2x_4)$. Next, we write the equation for $d(x_1^2 + x_2^2)/dt$ (this derivative being known from previous steps), and note that all quantities on the right hand side are known except the last term $2x_2V_s/\pi L$; now we have two choices - either V_s is the third input (in which case we pick the third output $y_3 = x_2$), or V_s is a known constant, so we can determine x_2 (and x_1 from the known magnitude of the tank current). The first two equations in (2) are linear and decoupled in terms of the remaining unknowns x_3 and x_4, and thus easily solvable.

ACKNOWLEDGMENTS

AMS gratefully acknowledges support by the National Science Foundation under grants ECS-9410354 and ECS-9502636, and by the ONR under grant 14-95-1-0723.

REFERENCES

[1] S.R. Sanders, J.M. Noworolski, X.Z. Liu and G.C. Verghese, "Generalized Averaging Method for Power Conversion Circuits," *IEEE Transactions on Power Electronics,* Vol. 6, No. 2, April 1991, pp. 251–259.

[2] E.X. Yang, F.C. Lee and M.M. Jovanovic, "Small–Signal Modeling of Power Electronic Circuits Using Extended Describing Function Technique," *Proceedings of the Virginia Power Electronics Seminar,* Vol 4, September 1991, pp. 155–166.

[3] C.T. Rim and G.H. Cho, "Phasor Transformation and its Application to the DC/AC Analysis of Frequency Phase-Controlled Series Resonant Converters," *IEEE Transactions on Power Electronics,* Vol. 5, No. 2, April 1990, pp. 201–211.

[4] V. Vorperian, "Approximate Small-Signal Analysis of the Series and Parallel Resonant Converters," *IEEE Transactions on Power Electronics,* Vol. 4, No. 1, January 1989, pp. 15–24.

[5] M.G. Kim and M.J. Youn, "An Energy Feedback Control of Series Resonant Converters," *IEEE Transactions on Power Electronics,* Vol. 6, No. 3, July 1991, pp. 338–345.

[6] R. Oruganti, J.J. Yang and F.C. Lee, "Implementation of Optimal Trajectory Control of Series Resonant Converters," *IEEE Transactions on Power Electronics,* Vol. 3, No. 3, July 1988, pp. 318–327.

[7] M.E. Elbuluk, G.C. Verghese and J.G. Kassakian, "Sampled-Data Modeling and Digital Control of Resonant Converters," *IEEE Transactions on Power Electronics,* Vol. 3, No. 3, July 1988, pp. 344–354.

[8] S.R. Sanders, G.C. Verghese and D.E. Cameron, "Nonlinear Control of Switching Power Converters," *Control - Theory and Advanced Technology,* 1989, Vol. 5, No. 4, pp. 601–617.

[9] S.R. Sanders and G.C. Verghese, "Lyapunov-Based Control for Switching Power Converters," *Proc. IEEE PESC,* 1990, pp. 51-58.

[10] A.M. Stankovic, "A Dissipativity-Based Controller for Series Resonant DC/DC Converters," *Proc. IEEE PESC,* 1996, pp. 1844–1849.

[11] C.A. Jacobson, A.M. Stankovic ad G. Tadmor, "Design of Robust Controllers for Resonant DC/DC Converters," *Proc. IEEE Conference on Control Applications,* Albany, 1995, pp. 360–365.

[12] R. Ortega and G. Espinosa, "Torque Regulation in Induction Motors," *Automatica,* 1993, Vol. 29, No. 3, pp. 621-633.

[13] R.M. Murray, M. Rathinam and W. Sluis, "Differential Flatness of Mechanical Control Systems: A Catalog of Prototype Systems" *ASME Intl. Mech. Engr. Congress,* Nov. 1995. (Preprint).

[14] H. Sira-Ramirez, R. Ortega, P. Martin, P. Rouchon and R. Marquez "Regulation of DC/DC Power Converters: A Differential Flatness Approach," *Proc. IFAC World Congress,* San Francisco, July 1996, Vol. 2b-17, pp. 43-48.